

## FORECASTING CAVITY PRESSURE AND TEMPERATURE IN AN INJECTION MOLDING PROCESS TOWARDS GREY MODELING

Rodolfo Gabriel Pabst <sup>1</sup>

Adriano Fagali de Souza <sup>2</sup>

Alexandro Garro Brito <sup>3</sup>

<sup>1,2,3</sup> Universidade Federal de Santa Catarina

<sup>1</sup> rodolfo.gabriel.pabst@posgrad.ufsc.br, <sup>2</sup> adriano.fagali@ufsc.br, <sup>3</sup> alexandro.brito@ufsc.br

**Abstract.** Today, the injection molding is one of the most important processes to manufacture plastic parts. Because it has a nonlinear and time varying behavior, existing process control approaches are based in model-based predictive procedures. Usually, these procedures require a previous knowledge about the process dynamics, what complicates its modeling. In the present work, a simple approach based on grey models is treated. It does not require previous information about the process. A regularized least squares method was used to adjust the model, resulting in a fast identification procedure, robust to ill-conditioning in the estimates. The model was validated using experimental data obtained during injection molding processes where the seasonal differenced cavity temperature varied along 2.56 °C and the cavity pressure varied along 13.85 MPa. The pressure and temperature signals inside the cavity could be forecasted with mean absolute deviations of 0.1708 °C and 0.6607 MPa.

**Keywords:** Injection molding. Grey modeling. Forecasting. Regularization theory. Process variables

### 1. INTRODUCTION

The injection molding is a multi-stage batch process, being the most employed method on manufacturing plastic parts. The quality of the injected parts is influenced by process and machine variables. The first kind corresponds to signals measured within mold cavity (e. g., cavity pressure and temperature), while the second one comprises hydraulic machinery and injection unit variables (e.g., reciprocating screw stroke and the molten temperature in the injection cannon).

Process variables exhibit a closer correlation with the part quality, since transfer phenomena during injection molding are dependent on the cavity geometry. Studies on this subject can be find in Kuo and Jeng (2010) and in Kovács and Sikló (2011). The first one evaluated the effect of the cross-sectional cavity dimension on the tensile properties of the injected parts. It was concluded, after experiments, that in thicker parts the heat generated by viscous dissipation increase the occurrence of molecular bonds and self-diffusion phenomenon. Kovács and Sikló (2011) demonstrated, through simulation on Autodesk Moldflow, the occurrence of defects caused by non-homogeneous cooling in sections with angular profile. The asymmetric cooling was caused by temperature differences between the two halves of the mold. The relation between the part morphology and process variables was also investigated by Nam *et al.* (2016). The authors modelled morphological errors on injected lens as a surface response in function of cavity pressure and temperature.

The information in the process variables is very useful on monitoring and controlling the injection molding. However, the process is nonlinear, time varying and may exhibit significant time delays between process variables and machine variables (usually employed as manipulated variables in control approaches). As a consequence, a wide range of operating conditions can occur and constant parameters controllers may present poor performance due to model uncertainties (Yang and Gao, 2013). In order to avoid this issue, predictive control approaches based on adaptive models are employed.

Predictive controlling of process variables are described in Zou *et al.* (2018) and in Hopmann *et al.* (2017), while the predictive controlling of machine variables is presented by Froelich *et al.* (2019). Other techniques that usually present good performance as well are based on self-tuning regulators with parameters estimated by least squares methods with finite-time forgetting window. However, these approaches require a previous knowledge about the system dynamics with the aim of determining the rate which the model adapt to the process. A fast rate can jeopardize the process estimates for noisy signals, while a slow rate may not track fast parameter variations (Yang and Gao, 2013).

The current work presents a model developed for forecasting the pressure and temperature in an injection molding process. It is proposed a procedure which does not require previous knowledge about the system dynamics. This is based on grey modeling, which represent small growing sequences as exponential profiles. The grey model's parameters can be calculated at each sampling interval through least squares estimators. The main advantage of this approach is the possibility to make predictions even when the data is scarce and with a high degree of uncertainty (Liu *et al.*, 2017). In the present approach, only the modeling of the process was treated, since the process variables control would require

modifications in the injection molding machine. Experimental data was acquired (pressure and temperature) during an injection molding process to validate the proposed model.

## 2. METHODOLOGY

The current work presents a grey model developed to predict pressure and temperature signals inside a mold cavity, during the injection molding process. The proposed model was evaluated using data of a real batch of injected plastic parts. To do so, a mold was designed and manufactured and temperature and pressure sensors were installed in its cavity.

Although the closed loop control of process variables was not treated in this work, the modeling approach was done assuming this future application. Thus, controllable pressure and temperature signals were chosen to be identified. According to Michaeli and Schreiber (2009), several characteristics of the injected part, such as weight, morphology, sinking and warping, are defined by the cavity pressure. The cavity temperature is associated with the part dimensional accuracy as well, since its value at the end of holding stage determines the time required to cool the parts (Wang, 2012). However, due to a higher degree of inertia of the machine variables in relation to the cavity temperature, the last one cannot be controlled within an injection cycle.

According to Gao *et al.* (1993), it is possible to define a variable representative of the process to be controlled instead of the cavity temperature profile. This procedure is valid because the cavity temperature presents a periodic behavior in steady state. The authors proposed the cycle average temperature, the peak temperature and the partial cooling time (i. e., the time from the beginning of a cycle to the time when the profile assumes a predetermined value) as controllable variables. In the present work, it was adopted the seasonal differenced temperature:

$$\nabla_s T_t = T_t - T_{t-s} \quad (1)$$

where  $s$  is the number of sampling intervals in one injection cycle. Since the variable  $\nabla_s T_t$  represent a process deviation between two consecutive cycles, it is directly related to the process repeatability. So, its control can ensure the decreasing of the process variance along the injection cycles.

### 2.1 Grey modeling

Grey modeling is based on approximating accumulated sequences by first order ordinary differential equations. According to Liu *et al.* (2017), given a nonnegative and approximately smooth sequence  $x_t^{(0)}$ , it is possible to obtain a growing sequence  $x_t^{(1)}$  through the accumulating generation operator (AGO):

$$x_t^{(1)} = \text{AGO} \left( x_t^{(0)} \right) = \sum_{i=1}^t x_i^{(0)} \quad (2)$$

The original sequence can be recovered through the inverse accumulating generation operator (IAGO):

$$x_t^{(0)} = \text{IAGO} \left( x_t^{(1)} \right) = x_t^{(1)} - x_{t-1}^{(1)} \quad (3)$$

The grey model GM(1, 1) was formerly proposed by Deng (1982) in terms of a development index  $-a$  and of a grey actuating quantity  $b$ :

$$\frac{dx_t^{(1)}}{dt} + ax_t^{(1)} = b \quad (4)$$

The notation GM( $r, h$ ) indicates a  $r$ -th order model with  $h - 1$  exogenous variables. The present work treated only the grey model GM(1, 1). However, Eq. (4) requires  $x_t^{(1)}$  to exhibit exponential growing pattern, and this only occurs when the stepwise ratio  $\sigma_t = x_t^{(1)}/x_{t-1}^{(1)}$  is constant. To deal with that, an approach used as theoretical foundation to the grey modeling is the quasi-exponential condition. Liu *et al.* (2017) define the quasi-exponential condition such that  $\sigma_t \in [\sigma_{min}, \sigma_{max}]$ ,  $\sigma_{max} - \sigma_{min} < 0.5$ . Thus, the AGO operator is applied to the original sequence until the quasi-exponential condition is fulfilled. Usually, one accumulation is sufficient, justifying the use of a first order grey model.

The continuous time model in Eq. (4) is defined by Liu *et al.* (2017) as the *whitenization* of the autoregressive model:

$$x_t^{(0)} + az_t^{(1)} = b \quad (5)$$

where  $z_t^{(1)} = (x_t^{(1)} + x_{t-1}^{(1)})/2$  is the moving average of the accumulated sequence. The parameters  $\vec{\theta} = [a \ b]^t$  can be obtained by a least squares estimator:

$$\hat{\theta} = (B^t B)^{-1} B^t \vec{y} \quad (6)$$

where:

$$B = \begin{bmatrix} -z_2^{(1)} & -z_3^{(1)} & \dots & -z_t^{(1)} \\ 1 & 1 & \dots & 1 \end{bmatrix}^t, \vec{y} = [x_2^{(0)} \ x_3^{(0)} \ \dots \ x_t^{(0)}]^t \quad (7)$$

Thus, it is possible to predict the next value of the time series through the solution of Eq. (4):

$$\begin{cases} \hat{x}_{t+1}^{(1)} = (x_1^{(0)} - a/b)e^{-at} + a/b \\ \hat{x}_{t+1}^{(0)} = \hat{x}_{t+1}^{(1)} - x_t^{(1)} \end{cases} \quad (8)$$

with parameters  $\hat{\theta}$  given by Eq. (6). Although the estimator  $\hat{\theta}$  is optimal, it is necessary the matrix  $B^t B$  to be invertible in order to avoid unstable numerical results. When this happens, the inversion is said ill-conditioned.

Given a mapping  $\vec{y} = F(\vec{x})$ ,  $F : \mathbb{X} \rightarrow \mathbb{Y}$ , its reconstruction is said well-conditioned if the functional  $F(\vec{x})$  satisfy all of the three conditions postulated by Hadamard (1902) apud Haykin (2008):

- Existence: for each  $\vec{x} \in \mathbb{X}$  there exist a  $\vec{y} \in \mathbb{Y}$ ;
- Uniqueness: for each pair  $\vec{x}_1, \vec{x}_2 \in \mathbb{X}$ ,  $F(\vec{x}_1) = F(\vec{x}_2)$  if and only if  $\vec{x}_1 = \vec{x}_2$ ;
- Continuity: for each  $\varepsilon > 0$  there exist a  $\delta = \delta(\varepsilon)$  such that a metric  $\rho_{\mathbb{X}}(\vec{x}_1, \vec{x}_2) < \varepsilon$ , induced on  $\mathbb{X}$ , implies that  $\rho_{\mathbb{Y}}(F(\vec{x}_1), F(\vec{x}_2)) < \delta$ , being  $\rho_{\mathbb{Y}}(\cdot, \cdot)$  a metric induced on  $\mathbb{Y}$ .

When at least on of these conditions is violated the reconstruction problem is ill-conditioned. According to Haykin (2008), when the noise in the samples is too high, the existence and continuity conditions cannot be satisfied. However, these issues are not likely to happen in grey modeling, since the AGO operation attenuates the random component in the sequences (Liu *et al.*, 2017). On the other hand, uniqueness issues are reasonable when the sequence  $x_t^{(0)}$  is very close to zero.

Manipulating Eq. (6), it is possible to show that the parameters  $\hat{\theta}$  are given by:

$$\hat{a} = \frac{\sum_{i=2}^t z_i^{(1)} \sum_{i=2}^t x_i^{(0)} - (t-1) \sum_{i=2}^t z_i^{(1)} x_i^{(0)}}{(t-1) \sum_{i=2}^t (z_i^{(1)})^2 - (\sum_{i=2}^t z_i^{(1)})^2} \quad (9)$$

$$\hat{b} = \frac{\sum_{i=2}^t x_i^{(0)} \sum_{i=2}^t (z_i^{(1)})^2 - \sum_{i=2}^t z_i^{(1)} \sum_{i=2}^t z_i^{(1)} x_i^{(0)}}{(t-1) \sum_{i=2}^t (z_i^{(1)})^2 - (\sum_{i=2}^t z_i^{(1)})^2} \quad (10)$$

Thereby, when the sequence  $z_t^{(0)}$  assumes very small values, we have  $(t-1) \sum_{i=2}^t (z_i^{(1)})^2 \rightarrow (\sum_{i=2}^t z_i^{(1)})^2$  and the least squares estimator is numerically unstable. This corresponds to an eigenvalue very close to zero in the matrix  $B^t B$ , implying in a system with no unique solution in the limit when the minimum eigenvalue is zero.

Furthermore, according to Liu *et al.* (2017), the grey model GM(1, 1) becomes invalid when  $|a| \geq 2$ . From Eq. (5) we can deduce the difference equation:

$$x_t^{(1)} = \frac{1-a/2}{1+a/2} x_{t-1}^{(1)} + \frac{b}{1+a/2} \quad (11)$$

whose solution is:

$$x_t^{(1)} = (x_1^{(1)} - b/a) \left( \frac{1-a/2}{1+a/2} \right)^t + b/a \quad (12)$$

But, as far as  $x_1^{(1)} = x_1^{(0)}$ , the following solution to  $x_t^{(0)}$  can be obtained through the IAGO operator:

$$x_t^{(0)} = \left( \frac{b - ax_1^{(0)}}{1 + a/2} \right) \left( \frac{1 - a/2}{1 + a/2} \right)^t = C \left( \frac{1 - a/2}{1 + a/2} \right)^t \quad (13)$$

where  $C$  is a constant depending on the model parameters and on the initial value of  $x_t^{(0)}$ . According to Liu *et al.* (2017), the solution in Eq. (13) equals to a second order approximation, given by a McLaurin series, of the exponential function  $Ce^{at}$ . However, its domain of convergence is  $(-2, 2)$  since  $x_t^{(0)} \rightarrow \infty$ , when  $a = -2$ , and  $x_t^{(0)} = 0$ , when  $a = 2$ .

With the aim to avoid ill-conditioning in the grey modeling, regularization theory results were used. In regularization theory, solutions to ill-conditioned problems are stabilized by means of a nonnegative functional, which add previous information about the solution (Haykin, 2008). Therefore, the minimized quantity is the Tikhonov functional:

$$\varepsilon(F) = \varepsilon_s(F) + \lambda \varepsilon_c(F) \quad (14)$$

where  $\varepsilon_s(F)$  is a standard least squares cost function and  $\varepsilon_c(F) = \frac{1}{2} \|\mathbf{D}F\|^2$  is a regularization term given in terms of a linear differential operator  $\mathbf{D}$ . The parameter  $\lambda$  is a real nonnegative number called regularization parameter. When  $\lambda \rightarrow 0$ , the solution is completely determined by the samples, coinciding with the least squares estimator. When  $\lambda \rightarrow \infty$ , the solution is completely determined by the restriction imposed by the operator  $\mathbf{D}$ . Typically, the regularization parameter assumes nonzero finite values (Haykin, 2008).

In this work, the regularized least squares estimator:

$$\hat{\theta} = (B^t B + \lambda I) B^t \vec{y} \quad (15)$$

where  $I$  is the identity matrix, was employed. The estimator in Eq. (15) minimizes the following functional proposed by Tikhonov (1963):

$$\varepsilon(\vec{\theta}) = \|\vec{y} - B\vec{\theta}\|^2 + \lambda \|\vec{\theta}\|^2 \quad (16)$$

Denoting the biggest eigenvalue of the matrix  $B^t B$  as  $\lambda_{max}\{B^t B\}$  and the spectral norm of  $B$  as  $\|B\| = \sqrt{\lambda_{max}\{B^t B\}}$ , it is possible to say that the eigenvalues of the matrix  $B^t B + \lambda I$  fall in the interval  $[\lambda, \lambda + \|B\|^2]$ . So, the ill-conditioning can be reduced by increasing the regularization parameter. Besides that, the functional  $\varepsilon(\vec{\theta})$  also minimizes the quadratic norm  $\|\vec{\theta}\|^2$ , preventing the parameter  $a$  to assume excessive values.

## 2.2 Process variables measurement

An experimental mold was implemented to investigate the injection molding. Figures (1.a) and (1.b) present the part and the mold CAD geometry. This a mold of direct injection of cold runner type for thermoplastics processing. The cooling system has two U shaped channels with 8 mm of diameter at 18 mm of the cavity surface. The injection channel has 82 mm of length and a conical geometry with extremity diameters of 4.0 and 6.5 mm (close to the part), inserted at the center of the part geometry, resulting in the radial filling of the cavity. The parts, made of polypropylene H105, with 140 mm of diameter and 2 mm of width were injected in a HAITIAN SA1200/410 injection molding machine with screw diameter of 40 mm, injection load of 214 cm<sup>3</sup> and clamping force of 1200 kN.

A Kistler 6190CA sensor was used to measure the cavity pressure. This is a piezoelectric sensor and can be in direct contact with the molten polymer. A Kistler 5139A221 charge amplifier, connected to an Agilent 34970 data acquisition device, was used to transduce the voltage signal. Figure (1.d) shows the sensor positioned at 22 mm of the injection channel. The cavity temperature was measured by four K-type thermocouples, whose positions are indicated in Fig. (1.c). The temperature and pressure signals were both sampled at 5.43 Hz.

## 2.3 Evaluation of the models

With the aim to compare the results of the current work with literature results, the works of Zhao and Gao (1999), Zhao *et al.* (2014) and Zhang *et al.* (2019) were addressed. Although Hopmann *et al.* (2017) developed an adaptive model to cavity pressure, their results were based on a closed loop process, where disturbances are attenuated through the feedback of an error signal. Since the current work is based on an open loop process, the aforementioned works were taken as comparison references. These approaches, explained ahead, were based in static models of the process variables. In this sense, the grey modeling represents an improvement by addressing the dynamics of the process, consequently allowing

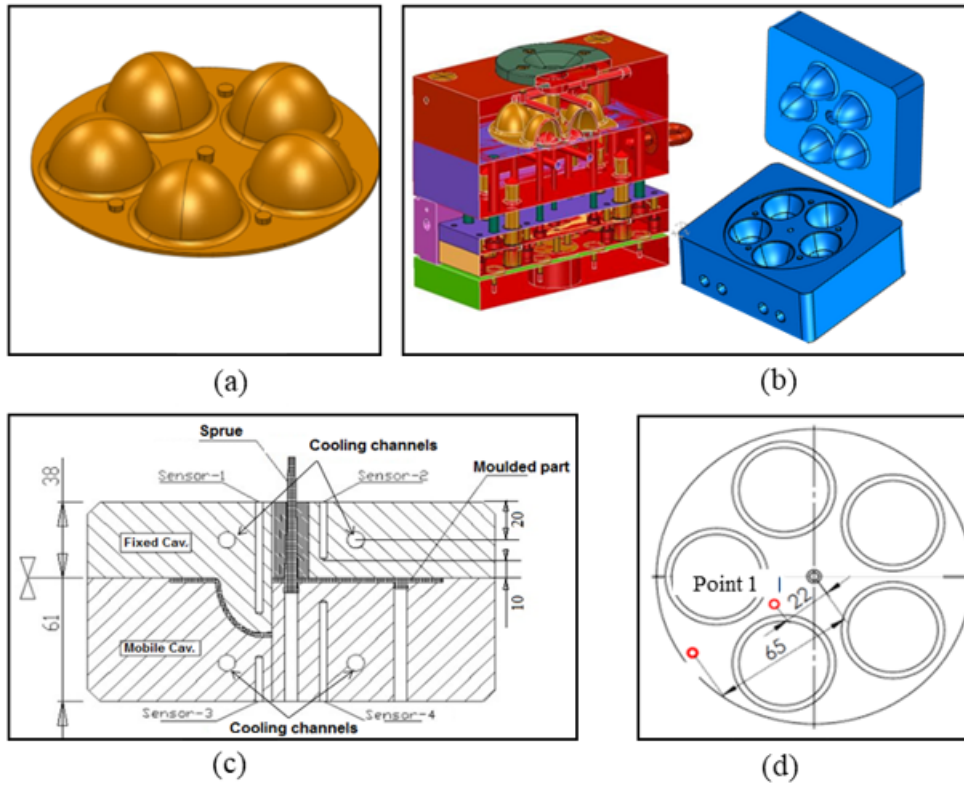


Figure 1: a) Part geometry; b) mold geometry; c) temperature sensors positions; and d) pressure sensor position.

further developments of closed loop control procedures.

Zhao and Gao (1999) used an artificial neural network (ANN) to model the functional relation between nozzle temperature and reciprocating screw stroke in a polypropylene injection molding process. The network was trained to 25 sets of experimental conditions through 10 thousand epochs, reaching a global error of 0.1%. By reconstructing the temperature profile through a piece-spline method it was possible to obtain estimates with maximum error below 2 °C.

An ANN-based approach was also employed by Zhao *et al.* (2014) to model cavity pressure. To train the ANN, cavity pressure (measured with a 6190A Kistler sensor) was used as the desired output of the network, whereas the hydraulic pressure, the cavity temperature and a reflection coefficient were used as its inputs. This reflection coefficient was given by the ratio between the incident and the reflected amplitudes of ultrasounds pulsed into the mold cavity. By training the ANN with 10 sets of data it was possible to achieve a maximum error of 0.6 MPa.

The approach proposed by Zhang *et al.* (2019) is based on the elongation of the machine's tie bars due to the cavity pressure. According to the sonoelasticity theory, there is a proportional relation between the stress on the tie bar and the time required to a pulsed ultrasound to be reflect at its ends. The method was calibrated with a 6157B Kistler sensor, yielding a determination coefficient of  $R^2 = 0.99962$  and relative error of 4.3%.

In this work, the cavity pressure  $p_t$  and the seasonal differenced temperature  $\nabla_s T_t$  signals were obtained through measurements in a mold cavity during a injection molding process. These samples were used to adjust models, whose performance was evaluated through the mean absolute deviation (MAD), the mean squared error (MSE) and the mean absolute percentage error (MAPE). These metrics are defined by:

$$\text{MAD} = \frac{1}{n} \sum_{t=1}^n |x_t - \hat{x}_t|, \text{MSE} = \frac{1}{n} \sum_{t=1}^n (x_t - \hat{x}_t)^2, \text{MAPE} = \frac{1}{n} \sum_{t=1}^n \frac{|x_t - \hat{x}_t|}{x_t} \quad (17)$$

where  $\hat{x}_t$  and  $x_t$  are the predicted and the real values, respectively. The metric MAPE measure, in percent, the prediction accuracy, while MAD and MSE are measures of the average magnitude of the forecast errors. The latter one imposes a major penalty on a larger error than a significant amount of small errors. Thereby, while the MSE measure has a close relationship with error peaks, the MAD measure is associated with homogeneous average over the forecast errors.

Injection molding processes present significant differences between them in terms of material properties, mold cavity geometries and employed injection molding machines. Thereby, the comparison with the results in previous works is very limited. The MAD, MSE and MAPE measures were compared with literature results in terms of their orders. For example, the values  $1.0 \times 10^{-1}$  and 1.0 have orders -1 and 0, respectively. Following the scientific notation, it was attempted to find results close or below to the presented in the literature.

### 3. RESULTS AND DISCUSSION

Figure (2) presents temperature and pressure time series measured in mold cavity. Since all the temperature signals presented similar profiles, only the time series with largest variance was used in grey modeling. It was observed to the time series sampled by the sensor in position 2 (Fig. (1)). In this process, each part is injected in a interval of 17.664 s, resulting in a periodicity of 96 sampling intervals. Thus, the seasonal differenced temperature  $\nabla_{96}T_t$  was modelled by the grey model GM(1, 1).

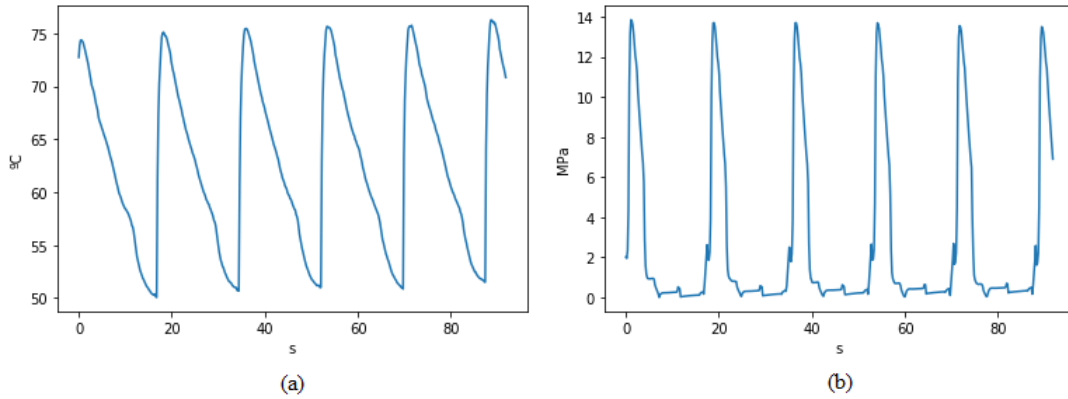


Figure 2: a) Cavity temperature and b) cavity pressure signals.

The evolution of the parameter  $a$  in the temperature model is presented in Fig. (3). The model becomes invalid in many instants of time when a null regularization parameter is used, as can be seen in Figure (3.a). It happens because the development index assumes values with modulus greater than two. However, this issue can be fixed by setting the regularization parameter to 0,01. Figure (3.b) shows that the parameter  $a$  falls within the interval  $(-2, 2)$  most of the time when the regularized estimator is used.

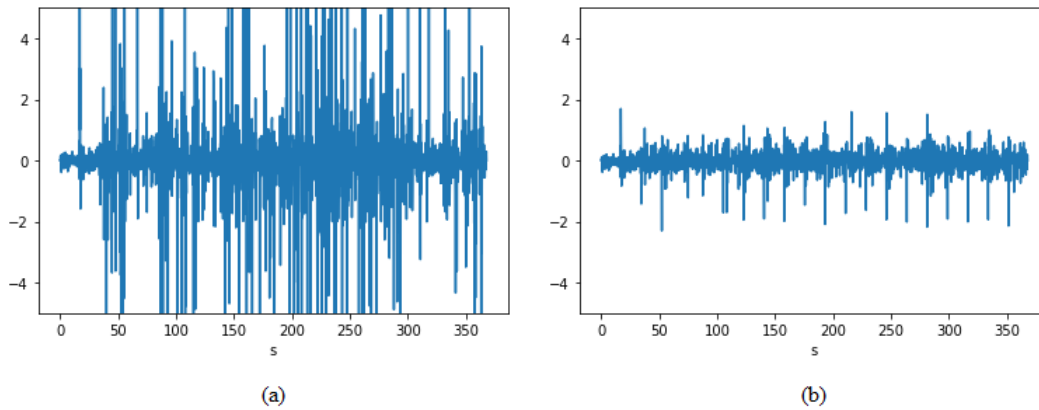


Figure 3: Parameter  $a$  evolution with regularization parameter a)  $\lambda = 0$  and b)  $\lambda = 0.01$ .

In the pressure model, the coefficients were adjusted by a ordinary least squares estimator since no ill-conditioning was observed. Being defined the process variables and the estimator, the grey models were adjusted. In both cases, the grey model GM(1, 1) was fitted to sequences with three samples. Figure (4) exhibit the forecasts (red dashed lines) together with the real values (blue full lines). Visually, the predictions presented good agreement with the sampled data, with large errors occurring only during a few instants of time. In pressure forecasting this occurs during the packing pressure peak, due to the change in the signal trend, reaching values above 10 MPa during the packing stage.

By applying the MAD and MSE measures proposed in Eq. (17) to the temperature forecast, the results  $1.708 \times 10^{-1}$  °C and  $4.018 \times 10^{-1}$  °C<sup>2</sup> were found. The measures presented the same order, being in accordance with the low magnitude of the peaks in the time series. The MAPE measure, however, diverged due to values very close to zero in the time series. As can be seen in Eq. (17) the terms in the sum of MAPE measure are inversely proportional to the real values of the time series. The errors measures were also calculated when  $\lambda = 0$ . The MAD and MSE measures presented excessive values ( $1.046 \times 10^{13}$  °C and  $4.478 \times 10^{28}$  °C<sup>2</sup>) and the MAPE measure diverged again. This results demonstrate the good performance of the regularized estimator on identifying the process.

Although it is not possible to compare the current results with the presented by Zhao and Gao (1999) in terms of

relative error, it is possible to establish a comparison based on MAD and MSE. As can be seen in Fig. (4), the spreading of the forecasts around the real values is very low, except for a few points. Taking the  $MSE = 4.018 \times 10^{-1} \text{ } ^\circ\text{C}^2$  as a measure of this variance, it is possible to say that most of the errors occur below  $1 \text{ } ^\circ\text{C}$ , which has the order 0, like in the as the results of Zhao and Gao (1999). This assumption is corroborated by the MAD measure of  $0.1708 \text{ } ^\circ\text{C}$ .

The error measures associated with the pressure forecasting were  $MAD = 6.607 \times 10^{-1} \text{ MPa}$ ,  $MSE = 3.513 \text{ MPa}^2$  and  $MAPE = 59.41\%$ . The first one was a better indicative of the forecasting performance, since MSE and MAPE measures were compromised by the error peaks and by the low pressure values observed in the deadtimes after the part ejection. These deadtimes continue until the molten polymer reaches the pressure sensor in the next injection cycle. The use of regularized estimators did not result in better accuracy keeping the measures close to the observed by the ordinary least squares estimator.

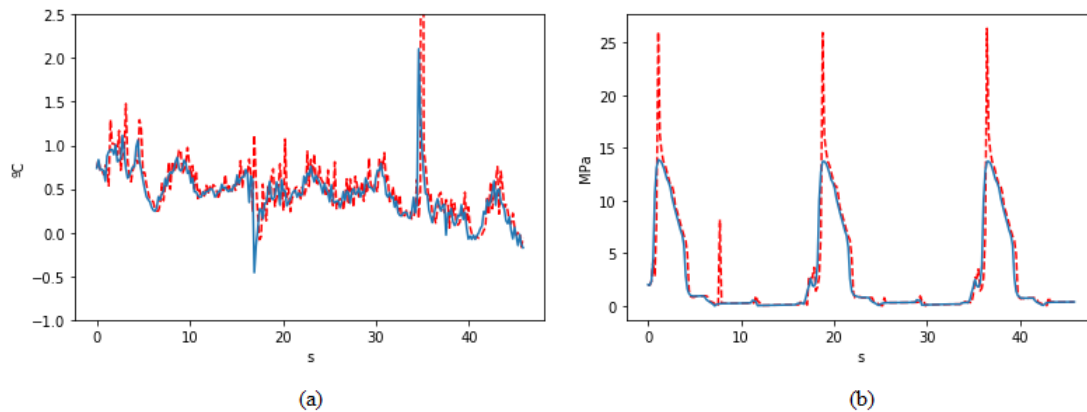


Figure 4: a) Seasonal differenced temperature  $\nabla_{96}T_t$  and b) cavity pressure  $p_t$  forecasting.

The MAD measure for pressure forecasting ( $0.6607 \text{ MPa}$ ) has the same order of the maximum error ( $0.6 \text{ MPa}$ ) achieved by Zhao *et al.* (2014). However, the MSE measure ( $3.513 \text{ MPa}^2$ ) implies that the standard deviation of the forecasts around the real values is  $1.874 \text{ MPa}$ . To verify the contribution of the seasonal peaks on the error measures, they were calculated again neglecting errors with absolute value higher than  $2 \text{ MPa}$ . This resulted in a lower order to the MAD and MSE measures ( $1.608 \times 10^{-1} \text{ MPa}$  and  $1.018 \times 10^{-1} \text{ MPa}^2$ , respectively), while the  $MAPE = 26.87\%$  remained in the same order as before due to the contributions of the small pressure values during the deadtimes of the process. Thereby, the standard deviation from the real values ( $3.191 \times 10^{-1} \text{ MPa}$ ), as well as the MAD measure, presented the order -1, the same as the results of Zhao *et al.* (2014).

In order to compare the current results with the presented by Zhang *et al.* (2019), a determination coefficient was estimated to the pressure forecast. The comparison based on relative errors was not carried out since the MAPE measure showed to be inadequate in the current work. The errors associated with the seasonal peaks were neglect again, yielding an determination coefficient  $R^2 = 0.99207$ . Thus, approximately  $99,21\%$  of the variation in the forecasts is due to the variation on the real time series. This is very close to the result  $R^2 = 0.99962$  presented by Zhang *et al.* (2019).

#### 4. CONCLUSIONS

The present work evaluated the performance of grey models GM(1, 1) on injection molding process variables forecasting. The main results can be enumerated as:

- Low forecasting errors (MAD) of  $0.1708 \text{ } ^\circ\text{C}$  and  $0.6607 \text{ MPa}$  were obtained by using sequences with three samples.
- It is necessary to use a regularized estimator for the seasonal differenced temperature signal in order to avoid ill-conditioning.
- In temperature and pressure forecasting the MAD measure was more reasonable with the predictions performance.
- Based on MAD and MSE measures, the grey model forecasts presented accuracy close to the observed to static models forecasts in another open loop injection molding process.
- Grey modeling addresses the dynamics of the time series sequences, being an improvement to the aforementioned static modeling approaches.

Although the good results, there are another factors which may contribute with the modeling performance. The grey model GM(1, 1) ignores the possibility of autocorrelation between the forecasting errors, since the AGO operation reduces the randomness in the sequences. Moreover, the process variables may be correlated since temperature is related to the thermodynamic pressure by means of a equation of state. Thereby, the investigation on modeling the forecasting errors as a moving average process and temperature and pressure signals as covariables is proposed as a subject of future works.

## 5. ACKNOWLEDGEMENTS

Thanks to the Coordenação de Aperfeiçoamento de Pessoal de Nível Superior (CAPES) and to the Conselho Nacional de Desenvolvimento Científico e Tecnológico (CNPq) by the financial support on this research, to the plastic parts manufacturing company Sokit by the support on the experimental procedures used in this work and to the automation company Branqs by the assistance on the research project whose the present work belongs.

## 6. REFERENCES

- Deng, J.L., 1982. "Control problems of grey systems". *Systems & Control Letters*, Vol. 1, No. 5, pp. 288 – 294.
- Froelich, C., Kemmetmüller, W. and Kugi, A., 2019. "Model-predictive control of servo-pump driven injection molding machines". *IEEE Transactions on Control Systems Technology*, pp. 1 – 16.
- Gao, F., Patterson, W.I. and Kamal, M.R., 1993. "Dynamics and control of surface and mold temperatures in injection molding". *International Polymer Processing*, Vol. 8, No. 2, pp. 147 – 157.
- Haykin, S., 2008. *Neural Networks: A Comprehensive Foundation*. Prentice Hall. ISBN 9780131471399.
- Hopmann, C., Abel, D., Heinisch, J. and Stemmler, S., 2017. "Self-optimizing injection molding based on iterative learning cavity pressure control". *Production Engineering*, Vol. 11, No. 2, pp. 97 – 106.
- Kovács, J.G. and Sikló, B., 2011. "Investigation of cooling effect at corners in injection molding". *International Communications in Heat and Mass Transfer*, Vol. 38, No. 10, pp. 1330 – 1334.
- Kuo, H.C. and Jeng, M.C., 2010. "Effects of part geometry and injection molding conditions on the tensile properties of ultra-high molecular weight polyethylene polymer". *Materials & Design*, Vol. 31, No. 2, pp. 884 – 893.
- Liu, S., Yang, Y. and J, F., 2017. *Grey Data Analysis: Methods, Models and Applications*. Springer. ISBN 9789811094583.
- Michaeli, W. and Schreiber, A., 2009. "Online control of the injection molding process based on process variables". *Advances in Polymer Technology*, Vol. 28, No. 2, pp. 65 – 76.
- Nam, J.S., Na, C.R., Jo, H.H., Song, J.Y., Ha, T.H. and Lee, S.W., 2016. "Injection moulded lens form error prediction using cavity pressure and temperature signals based on k-fold cross validation". *Journal of Engineering Manufacture*, Vol. 232, No. 5, pp. 928 – 934.
- Tikhonov, A.N., 1963. "Solution of incorretly formulated problems and regularization method". *Soviet Mathematics: Doklady*, Vol. 4, pp. 1035 – 1088.
- Wang, J., 2012. *PVT Properties of Polymers for Injection Molding*. ISBN 9789535102977.
- Yang, Y. and Gao, F., 2013. "Feedback control". In H. Zhou, ed., *Computer Modeling for Injection Molding*, Wiley, Hoboken (USA), chapter 12, pp. 314 – 338.
- Zhang, J., Zhao, P., Zhao, Y., Huang, J., Xia, N. and Fu, J., 2019. "On-line measurement of cavity pressure during injection molding via ultrasonic investigation of tie bar". *Sensors and Actuators A: Physical*, Vol. 1, pp. 118 – 126.
- Zhao, C. and Gao, F., 1999. "Melt temperature profile prediction for thermoplastic injection molding". *Polymer Engineering and Science*, Vol. 39, No. 9, pp. 1787 – 18001.
- Zhao, P., Zhou, H., He, Y., Cai, K. and Fu, J., 2014. "A nondestructive online method for monitoring the injection molding process by collecting and analysing machine running data". *International Journal of Advanced Manufacturing Technology*, Vol. 72, No. 5 - 8, pp. 765 – 777.
- Zou, T., Wu, S. and Zhang, R., 2018. "Improved state-space model predictive fault-tolerant control for injection molding batch processes with partial actuator faults using ga optimization". *ISA Transactions*, pp. 1 – 7.

## 7. RESPONSIBILITY NOTICE

The authors are the only responsible for the printed material included in this paper.